Energy Conversion and Management 84 (2014) 305–310

Contents lists available at ScienceDirect

Energy Conversion and Management

journal homepage: www.elsevier.com/locate/enconman

# Cogeneration solar system using thermoelectric module and fresnel lens

M. Hasan Nia [a], A. Abbas Nejad [a,*], A.M. Goudarzi [b], M. Valizadeh [b], P. Samadian [c]

[a] Department of Mechanical Engineering, Shahrood University of Technology, P.O. Box 3619995161-316, Shahrood, Iran
[b] Department of Mechanical Engineering, Babol Nooshiravani University of Technology, Babol, Iran
[c] Director of Control Section AAA Linen, London, UK

ARTICLE INFO

*Article history:*
Received 18 August 2013
Accepted 13 April 2014
Available online 8 May 2014

*Keywords:*
Cogeneration
Thermoelectric
Fresnel lens
Preheated water
Electrical power

ABSTRACT

The main purpose of this paper is the experimental investigation of an electricity and preheated water cogeneration system by thermoelectric. In the presented design, Fresnel lens and thermoelectric module (TE module) were utilized in order to concentrate solar beam and generate electrical power, respectively. The energy of concentrated sunlight on the heat absorber of TE module is transferred to cold water reservoir. Heat transfer in TE module leads to temperature difference in its both sides and finally electrical power is generated. The main components of this system consist of a monoaxial adjustable structure, a thermoelectric generator (TEG) and a Fresnel lens with an area of 0.09 $m^2$. Results revealed that matched load output power is 1.08 W with 51.33% efficiency under radiation intensity of 705.9 $W/m^2$. In order to apply TE module capacity optimally for electrical generation, it is recommended to employ an array of Fresnel lenses which transfer heat to TE module by an intermediate fluid.



## 1. Introduction

Solar energy, which is categorized as a renewable energy, is known as an appropriate as well as clean source of energy. In the near future, this source of energy will be the main part of renewable energies and causes considerable reduction in consumption of fossil fuels. There are some strategies for solar energy application to generate heat and power, such as solar water heaters, photovoltaic and solar thermal power plants. However, lower energy density, seasonal accessibility and geographical dependence of solar energy are major challenges in identifying its suitable applications as a heat source. Consequently, exploring high efficiency solar energy concentration technology is necessary and realistic [1]. The mentioned problem is solved by employing Fresnel lens along with thermoelectric modules in this proposed solar system.

In contrast with other concentrating devices, Fresnel lenses have some advantages such as small volume, light weight, high optical quality and lower manufacturing and capital costs which make them one of the best options. The first attempts to use Fresnel lenses for solar energy collection occurred when suitable plastics such as polymethylmethacrylate (PMMA) became available in the 1950s. PMMA is resistant to sunlight, remains thermally stable up to at least 80 °C, its special transmissivity matches the solar spectrum, and its refraction index is 1.49, which is very close to that of glass [2]. Therefore, because of high optical quality and low cost of manufacturing technology, most of the Fresnel lens designers use this material to concentrate sunlight. Fresnel lenses have widespread applications in generating power from solar radiation [3], hydrogen generation [4], as well as solar-pumped laser [5].

Fresnel lens was investigated by Szulmayer [6,7] and Nelson et al. [8] for the first time. They designed an experimental system and achieved the temperature of 60–143 °C for water heating and vapor production. Their system's efficiency for solar collection was 50% with a geometric concentration ratio of 5 [6]. Besides, Hastings and Allums [9] studied plasticline- focus Fresnel lens. They succeeded in reaching 200–370 °C. Sierra and Vazquez [10–12] designed a concentrated system which could reach 1500–2000 °C in few minutes by the use of Fresnel lens. Temperature of the focused beam was so high that it caused ignition in the mixture of nickel aluminum.

In the recent two decades, thermoelectric modules (TE modules) were widely employed due to their advantages. These small devices are used to convert thermal to electrical energy without a rotating part, noise and vibrations. TE modules are known as a green technology and they are categorized as flexible sources due to their application range [13–16].

The optimum characteristics of flat-plate type solar energy collectors in combination with thermocouples were evaluated by Telkes [17]. Those characteristics were designed for maximum energy conversion. He obtained an efficiency of 0.63% by using flat-plate collectors with two glass panes. Calculations indicate

* Corresponding author. Tel.: +98 273 3392204; fax: +98 273 3300258.
*E-mail address:* abbasnejad@shahroodut.ac.ir (A. Abbas Nejad).

http://dx.doi.org/10.1016/j.enconman.2014.04.041
0196-8904/

**Nomenclature**

| | |
|---|---|
| $I$ | matched load output current (A) |
| $I_{FL}$ | radiation intensity on Fresnel lens (W/m$^2$) |
| $I_t$ | local radiation intensity (W/m$^2$) |
| $P_{\max}$ | matched load output power (W) |
| $\dot{Q}_W$ | thermal power transferred to water (W), $\dot{Q}_W = \dot{m}c_p(T_{\mathrm{wo}} - T_{\mathrm{wi}})$ |
| $T_c$ | thermoelectric cold side temperature (°C) |
| $T_h$ | thermoelectric hot side temperature (°C) |
| $T_{wi}$ | inlet water temperature (°C) |
| $T_{wo}$ | outlet water temperature (°C) |
| $\Delta T$ | temperature difference between hot side and cold side of thermoelectric (°C) |
| $\Delta T_w$ | temperature difference between inlet and outlet water (°C) |
| $V$ | matched load output voltage ($V$) |
| $\eta_e$ | electrical efficiency (%), $\eta_e = \frac{P_{\max}}{I_{FL}} \times 100$ |
| $\eta_{th}$ | thermal efficiency (%)), $\eta_{th} = \frac{\dot{Q}_w}{I_{FL}} \times 100$ |
| $\eta_{TEG}$ | thermoelectric generator efficiency (%), $\eta_{\mathrm{TEG}} = \frac{P_{\max}}{\dot{Q}_W + P_{\max}} \times 100\}$ |

that the efficiency may be increased to 1.05% by using four low-reflection panes.

Maneewan et al. [18] generated electrical power to drive an axial fan by means of a system consisting of roof solar collectors and TEG modules. They used a halogen lamp with varying power 400–1000 W to simulate solar radiation. 1.2 W power was achieved in a radiation intensity of 800 W/m$^2$ and an ambient temperature between 30–35 °C. Champier et al. [19] built and investigated an experimental prototype of biomass cook stoves. They designed a combustion chamber with high efficiency and put TE modules on two sides of the stove to generate 6 W electrical power from 4 TE modules. Nuwayhid et al. [20] examined a domestic wood stove experimentally. They used natural convection in thermoelectric in order to cool its cold side. Their results indicated that generated power on matched load state was 4.2 W for each TE module.

Kraemer et al. [21] designed a novel flat-panel solar thermal to electric power conversion technology based on the Seebeck effect and high thermal concentration. Their proposed system reached a maximum efficiency of 4.6% under 1 kWm$^{-2}$ conditions which was eight times higher than the previous studies.

He et al. [22,23] described a solar heat pipe thermoelectric generator (SHP-TEG) unit consists of an evacuated double-skin glass tube, a finned heat pipe and a TEG module.

Omer and Infield [24] employed a theoretical model of a thermoelectric device for evaluation of an optimum device in power generation mode. They compared four different thermoelectric modules using their proposed model. They also designed a two stage solar concentrator for combined heat and thermoelectric power generation. Their results indicated improvement in the concentration efficiency and overall performance of the solar concentrator [25].

Thermal and electrical performances of the concentrator, receiver and thermoelectric module were studied by Atik [26]. The surface temperatures, electric power and system efficiency were determined for different radiation intensity and concentration ratios.

Xiao et al. [27] established a three-dimensional finite element model of thermoelectric module based on low and medium temperature thermoelectric materials with temperature dependent properties.

Theoretical efficiency of STEGs was studied by Chen [28]. He purposed a model including thermal and optical concentrations. He concluded that the device efficiency increases but the opto-thermal efficiency decreases with increasing hot side temperature. Additionally, he pointed out that STEGs efficiency can be enhanced by operation in an evacuated environment.

Lesage et al. [29] investigated the thermopower of commercial thermoelectric modules under increasing electrical load 2conditions. They also applied this technique to a thermoelectric solar energy conversion using an artificial light source projected onto a solar vacuum tube.

In this research, the Fresnel is employed for concentrating solar beam on an oil reservoir which is used as heat transfer fluid. The absorbed heat is transferred to cold water in a heat exchanger to produce hot water. Also, thermoelectric generator (TEG) is employed in between Fresnel lens and cold water for power generation. The experimental results indicate the ability of the proposed system for cogeneration of heat and power (CHP).

## 2. Conceptual design

In this proposed design, solar radiation is concentrated by an array of Fresnel lenses in their focal points to increase radiation intensity. There are reservoirs full of oil at the center of each lens. The heat absorbed by the heat transfer fluid (mineral oil) transfers to water reservoir which is connected to TE module. The schematic design is shown in Fig. 1.

The set of TE module as well as oil and water reservoirs make a liquid–liquid heat exchanger which is depicted in Fig. 2.

## 3. Experimental setup

In this investigation, a TEG is located in the focal point of the Fresnel lens. Actually, this TEG is a liquid to liquid thermal heat exchanger which includes a TE module located in between two reservoirs full of oil and water, respectively. Fresnel lens concentrates sunlight on its focal point and enhances solar energy density in this zone. Fig. 3 shows a schematic of this experimental setup. Consequently, the oil temperature in the reservoir will increase. In order to expose the lens exactly under sun rays, an adjustable mechanical structure was considered.

The main components of this system consist of an iron frame which is monoaxial, a TEG, and a Fresnel lens. The Fresnel lens can be adjusted in an appropriate direction by changing the height of each screw in this structure. The size of this point-focus Fresnel lens is 30 × 30 cm$^2$.

The hot side of TE module is full of hot oil and water flows on the cold side with the rate of 0.002 kg/s. A thermoelectric power generation module based on $Bi_2Te_3$ (type TEP1-12656-0.6) was used in this system. The TEG module specifications are presented in Table 1. In order to reduce the heat loss by convection, TEG is located in a vacuumed glass bulb. In order to measure solar power radiation, a solar power meter (type: TES 1333R) is employed. Two types of thermometers are employed for temperature measurement, laser (Blue Gizmo model: BG 42) and thermocouple thermometer (Omni instrument model: Testo 91-1). Additionally, a voltmeter (Hioki

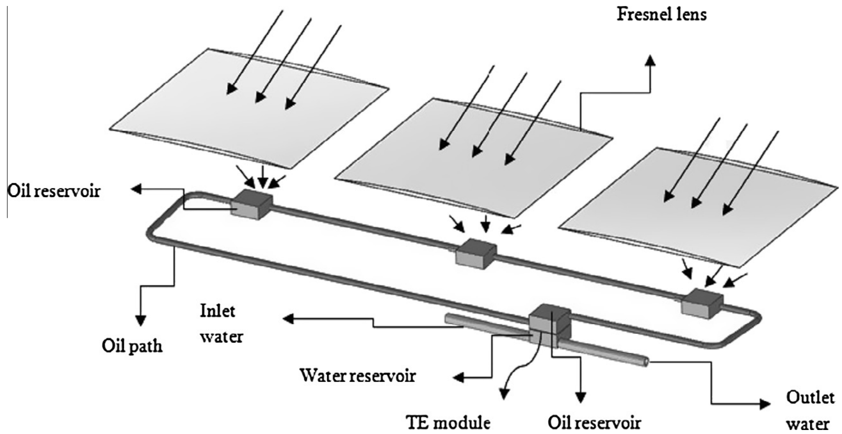


**Fig. 1.** Schematic of the proposed design.

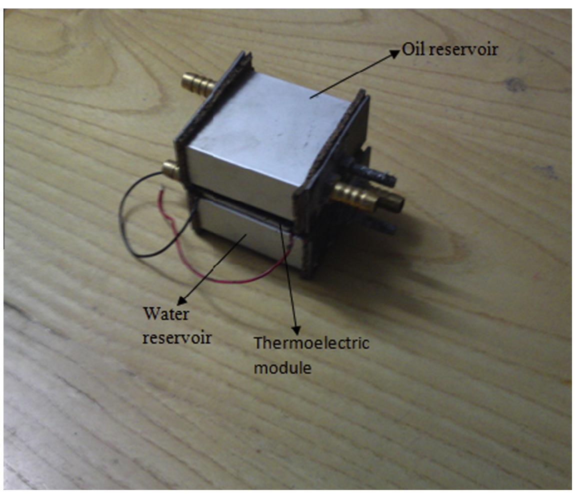


**Fig. 2.** Liquid–liquid heat exchanger equipped with TE module.

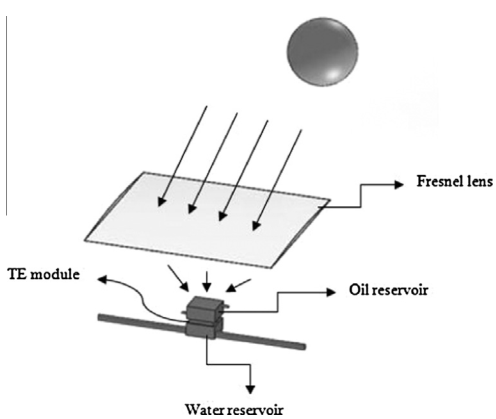


**Fig. 3.** Schematic of experimental setup.

3200) is employed to measure the generated voltage of thermoelectric. Specific heat capacity and density of the mineral oil used in this investigation at 25 °C are 2009.664 J/(kg K) and 0.883 g/cm$^3$, respectively. Fig. 4 shows the solar system built in this survey.

The experiments were carried out on 23rd, 24th, 27th August and 1st September 2012, in Babol, located in the north of Iran. (altitude: −2 m, latitude: 36.33, longitude: 52.41). Experiments were performed from 8 a.m. to 4 p.m. In order to decrease measurement errors, three different values for each data were registered.

**Table 1**
Specifications of TEG module.

| Property | Value |
|---|---|
| Size | 56 mm × 56 mm |
| Open circuit voltage (V) | 8.6 |
| Internal resistance (ohms) | 1.2 |
| Match load output voltage (V) | 4.2 |
| Match load output current (A) | 3.5 |
| Match load output power (W) | 14.7 |
| Heat flux across the module (W) | 350 |
| Heat flux density (W/cm$^2$) | 11 |
| Dimensionless figure of merit (ZT) | ~1 |

**Fig. 4.** Experimental solar system.

## 4. Results and discussion

At the first step, it is necessary to evaluate the maximum accessible temperature in oil reservoir while there is no fluid flow for heat transfer in the system. For this purpose, an experiment was carried out to evaluate the temperature of the oil reservoir's absorber surface on 23rd August at noon (maximum radiation intensity). The maximum attained temperature for the absorber surface was 130 °C. It is assumed that the temperature of the cold side of the thermoelectric remains 30 °C and heat flux due to sunlight is such

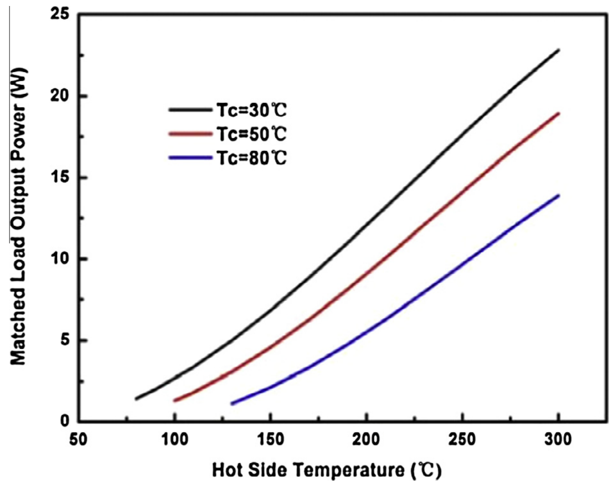


**Fig. 5.** Thermoelectric output power on matched load condition versus temperature [30].

**Table 2**
Recorded data on 24th August.

| Time | $T_h$ (°C) | $T_{wi}$ (°C) | $T_{wo}$ (°C) | $T_c$ (°C) | $\Delta T$ (°C) | $V$ (volt) | $I_t$ ($w/m^2$) | $I_{FL}$ ($w$) |
|---|---|---|---|---|---|---|---|---|
| 9 | 41.2 | 19.1 | 20.8 | 19.95 | 21.25 | 1.029 | 470 | 42.3 |
| 10 | 70.5 | 19.1 | 21.3 | 20.2 | 50.3 | 1.399 | 533.4 | 48 |
| 11 | 81.1 | 19.1 | 22.6 | 20.85 | 60.25 | 1.99 | 650.1 | 58.5 |
| 12 | 91.2 | 19.1 | 23 | 21.05 | 70.19 | 2.277 | 705.9 | 63.5 |
| 13 | 82.7 | 19.1 | 22.8 | 20.95 | 61.8 | 2.087 | 662.2 | 59.59 |
| 14 | 73.4 | 19.1 | 21.9 | 21.5 | 52 | 1.56 | 557.1 | 50.14 |
| 15 | 59.1 | 19.1 | 21.1 | 20.1 | 39.04 | 1.384 | 520.1 | 46.81 |
| 16 | 42.1 | 19.1 | 20.9 | 20 | 22.17 | 1.217 | 482.3 | 43.4 |

that the temperature of the hot side remains at 130 °C. According to Fig. 5, the maximum possible electrical power is about 6 W.

The potential of the designed system for cogenerating electricity and preheated water was investigated on three other days when water flow rate in reservoir was 0.002 kg/s. Typical recorded data on 24th August for a 7-h period of time are shown in Table 2.

### 4.1. Electrical power generation

The ability of the TE module's electrical power generation can be evaluated, according to measurements for the open circuit voltage of the module. Therefore, maximum reachable power from the module as well as circuit current intensity can be calculated. Besides, by considering radiation intensity on the Fresnel lens surface, electrical efficiency can be calculated.

The following equation is employed to determine the maximum power output obtained at the matched load [31].

**Table 3**
Calculated electrical data on 24th August.

| Time | $V$ (volt) | $I$ (A) | $P_{max}$ (Watt) | $I_{FL}$ (W/m$^2$) | $\eta_e$ (%) |
|---|---|---|---|---|---|
| 9 | 1.029 | 0.4286 | 0.2204 | 42.3 | 0.52 |
| 10 | 1.399 | 0.583 | 0.4078 | 48 | 0.85 |
| 11 | 1.99 | 0.8293 | 0.8253 | 58.5 | 1.41 |
| 12 | 2.277 | 0.9487 | 1.08 | 63.5 | 1.7 |
| 13 | 2.087 | 0.8695 | 0.9073 | 59.59 | 1.5 |
| 14 | 1.56 | 0.6499 | 0.5068 | 50.14 | 1.01 |
| 15 | 1.384 | 0.5766 | 0.399 | 46.81 | 0.8 |
| 16 | 1.217 | 0.507 | 0.3084 | 43.4 | 0.7 |

$$P_{max} = \frac{V_{oc}^2}{4R} \tag{1}$$

where $R$ is thermoelectric internal resistance (1.2 ohm) and $V$ is open circuit voltage for TE module. The electrical efficiency can be computed by:

$$\eta_e = \frac{P_{max}}{I_{FL}} \times 100 \tag{2}$$

where $P_{max}$ is the maximum thermoelectric generated power and $I_{FL}$ is the received radiated power on Fresnel lens surface. Calculated data for system on 24th August are shown in Table 3. As depicted in the table, the electrical efficiency of the system is too low. Due to the lens dimensions, the maximum achievable temperature without water cooling was 130 °C. It is recommended to use series arrangement of bigger lenses to attain higher electrical efficiency.

Generated electrical power on matched load condition for different radiation intensities during experiment is shown in Fig. 6.

As can be seen from Fig. 6, generated power is very low at the beginning and end of day due to lower solar radiation and low temperature of the thermoelectric hot side. Temperature of the thermoelectric hot side increases by increase in solar radiation until its maximum value at noon. As temperature difference between the hot side and the cold side increases, generated electrical power enhances. Results show that matched load electrical power during experiment was 1.08 W which is recorded at 12:00 p.m. on 24th August. Furthermore, total generated electrical energy can be obtained by integrating the electrical power over time which is 10.83, 9.8 and 9.78 kJ for 24th August, 27th August and 1st September, respectively.

### 4.2. Preheated water generation

In order to evaluate the ability of the system for generating preheated water, inlet and outlet water temperatures as well as water flow rate should be recorded. Moreover, by considering radiated power on the Fresnel lens surface, total thermal efficiency can be determined. Heat transfer rate to cooling water and thermal efficiency can be calculated by Eqs. (3) and (4), respectively.

$$\dot{Q}_w = \dot{m} c_p \Delta T_w \tag{3}$$

$$\eta_{th} = \frac{\dot{Q}_w}{I_{FL}} \times 100 \tag{4}$$

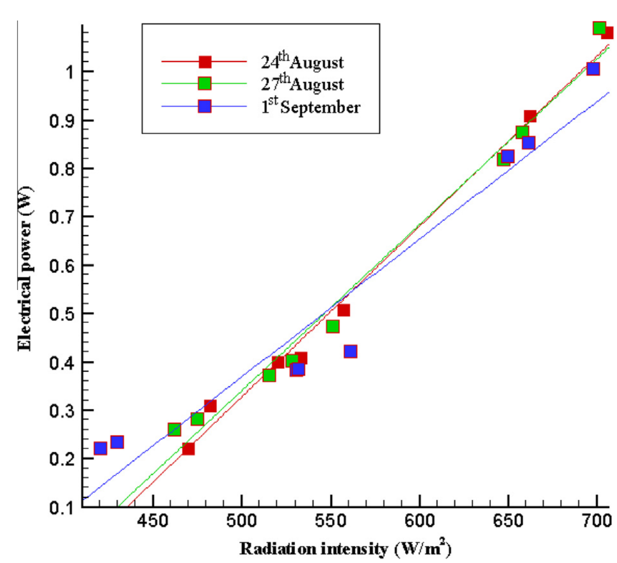


**Fig. 6.** Electrical power generated on matched load condition.

**Table 4**
Results of preheated water generating on 24th August.

| Time | $T_{wi}$ (°C) | $T_{wo}$ (°C) | $\Delta T_W$ (°C) | $\dot{Q}$ (W) | $\eta_{th}$ (%) | $\eta_{TEG}$ (%) |
|---|---|---|---|---|---|---|
| 9 | 19.1 | 20.8 | 1.7 | 14.21 | 33.6 | 1.52 |
| 10 | 19.1 | 21.3 | 2.2 | 18.39 | 38.31 | 2.17 |
| 11 | 19.1 | 22.6 | 3.5 | 29.26 | 50 | 2.74 |
| 12 | 19.1 | 23 | 3.9 | 32.6 | 51.33 | 3.2 |
| 13 | 19.1 | 22.8 | 3.7 | 30.93 | 51.9 | 2.84 |
| 14 | 19.1 | 21.9 | 2.8 | 23.4 | 46.66 | 2.11 |
| 15 | 19.1 | 21.1 | 2 | 16.72 | 35.71 | 2.33 |
| 16 | 19.1 | 20.9 | 1.8 | 15.04 | 34.65 | 2 |

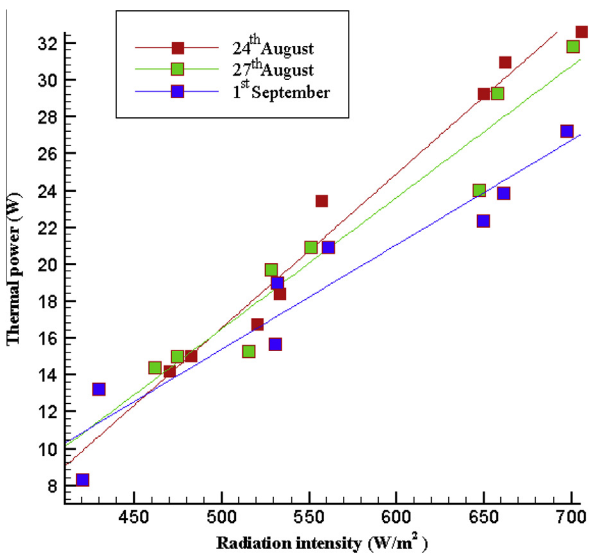


**Fig. 7.** Absorbed thermal power for different days of experiment.

**Table 5**
Calculated electrical power for different tests on 27th August.

| Hour | Test1 | Test2 | Test3 | Mean | Standard deviation | Uncertainty (%) |
|---|---|---|---|---|---|---|
| 9 | 0.251 | 0.262 | 0.266 | 0.260 | 0.008 | 3.045 |
| 10 | 0.411 | 0.400 | 0.393 | 0.401 | 0.009 | 2.178 |
| 11 | 0.825 | 0.810 | 0.813 | 0.816 | 0.008 | 0.956 |
| 12 | 1.011 | 1.048 | 1.053 | 1.037 | 0.023 | 2.204 |
| 13 | 0.87 | 0.886 | 0.863 | 0.873 | 0.012 | 1.357 |
| 14 | 0.459 | 0.481 | 0.473 | 0.471 | 0.011 | 2.279 |
| 15 | 0.366 | 0.375 | 0.371 | 0.371 | 0.004 | 1.178 |
| 16 | 0.283 | 0.280 | 0.281 | 0.281 | 0.001 | 0.526 |

**Table 6**
Calculated thermal power for different tests on 27th August.

| Hour | Test1 | Test2 | Test3 | Mean | Standard deviation | Uncertainty (%) |
|---|---|---|---|---|---|---|
| 9 | 14.2 | 14.4 | 14.5 | 14.367 | 0.153 | 1.063 |
| 10 | 19.7 | 19.5 | 19.7 | 19.633 | 0.115 | 0.588 |
| 11 | 23.5 | 24.1 | 24.37 | 23.99 | 0.445 | 1.856 |
| 12 | 31.9 | 31.6 | 31.8 | 31.767 | 0.153 | 0.481 |
| 13 | 29.4 | 29.1 | 29.3 | 29.267 | 0.153 | 0.522 |
| 14 | 16.9 | 16.6 | 17.1 | 16.867 | 0.252 | 1.492 |
| 15 | 15.5 | 15.1 | 15 | 15.2 | 0.265 | 1.741 |
| 16 | 12.1 | 11.6 | 12.1 | 11.933 | 0.289 | 2.419 |

The experiments were carried out for three days when the average ambient temperature and wind velocity were about 28 °C and 3 m/s, respectively. Thermal losses caused by environmental conditions such as ambient temperature and wind velocity were negligible due to locating the module in the vacuumed glass bulb. Table 4 shows the findings on 24th August. Results indicated that the maximum change in the temperature of inlet water is about 3.94 °C which was at 12:00 p.m. on 24th August. The hot outlet water in this system can be utilized in water heaters as preheated water in order to decrease fossil fuel consumption. Generated thermal power during a day is shown in Fig. 7 according to dates of experiments and radiation intensities.

According to Fig. 7, it is observed that as radiation intensity increases, absorbed thermal power will enhance due to solar concentration of the Fresnel lens.

Furthermore, by integrating the thermal power over time, it can be seen that total absorbed energy for water heating during experiments were 195.72, 190.53 and 183.5 kJ for 24th August, 27th August and 1st September, respectively.

In order To increase the accuracy of the results, solar radiation and output voltage has been recorded three times for each case. Table 5 and 6 show the calculated values, standard deviation and estimated uncertainties of the electrical and thermal powers for one day of experiments (27th August), respectively. Also, the mean values of electrical and thermal power with a 95% confidence interval are depicted in Figs. 8 and 9. It is obvious that the obtained results have very good accuracy.

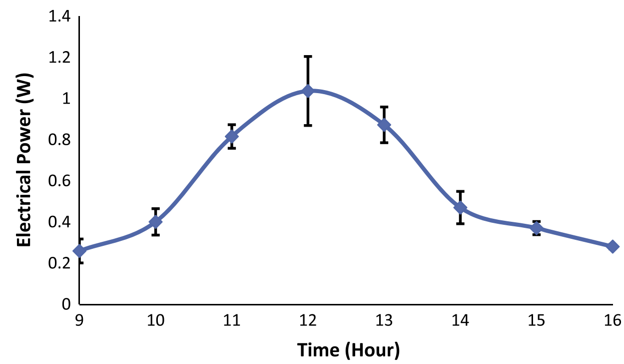


**Fig. 8.** Electrical power generated with 95% confidence interval.

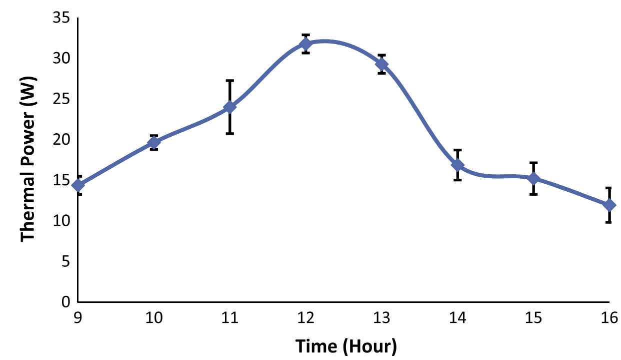


**Fig. 9.** Absorbed thermal power with 95% confidence interval.

## 5. Conclusion

A new cogeneration system is investigated experimentally by means of Fresnel lens and thermoelectric modules in order to generate electricity and thermal power.

Experimental results showed that the maximum available temperature on the oil reservoir surface was equal to 130 °C during three days of data recording.

Also, the maximum thermal efficiency during the mentioned experiments was about 51.9% which was recorded at 1:00 p.m. on 24th August. At this time, thermal power transferred to water was 30.93 W. Additionally, it was revealed that in case of utilizing water with a flow rate of 0.002 kg/s and an initial temperature of 19 °C, electrical power in matched load condition was 1.038 W.

According to recorded data as well as technical data in the TE module's user guide, it is recommended to use at least 6 lenses to achieve maximum electrical power (about 6 W) from one TE module.

The obtained results showed that the proposed arrangement can be widely used for different applications that need thermal and electrical power to reduce fossil fuel consumption and $CO_2$ emission.

## References


[1] Xiea WT, Daia YJ, Wanga RZ, Sumathy K. Concentrated solar energy applications using Fresnel lenses: a review 2011. Renew Sustain Energy Rev 2011;15(2011):2588–606.

[2] Leutz R, Suzuki A. Nonimaging Fresnel lenses: design and performance of solar concentrators. Heidelberg: Springer Verlag; 2001.

[3] O'Neil MJ, Piszczor MF, Eskenazi MI, McDanal AJ, George PJ, Botke MM. Ultra-light stretched Fresnel lens solar concentrator for space power applications. Proc SPIE 2003;5179:116–26.

[4] Alkan C, Sekerci M, Kunc S. Production of hydrogen using Fresnel lens-solar electrochemical cell. Int J Hydrogen Energy 1995;20(1):17–20.

[5] Ohkubo T, Yabe T, Yoshida K, Uchida S, Funatsu T, Bagheri B, et al. Solar-pumped 80 W laser irradiated by a Fresnel lens. Opt Lett 2009;34(2):175–7.

[6] Szulmayer W. Solar strip concentrator. Sol Energy 1973;14(3):327–35.

[7] Szulmayer W. Solar concentrator, US Patent, No. 4, 230, 094; 1980.

[8] Nelson DT, Evans DL, Bansal RK. Linear Fresnel lens concentrators. Sol Energy 1975;17(5):285–9.

[9] Hastings LJ, Allums SL. Performance characteristics of a 1.8 m × 3.7 m Fresnel lens solar concentrator. J Energy 1979;3(2):65–6.

[10] Sierra C, Vazquez AJ. High solar energy concentration with a Fresnel lens. J Mater Sci 2005;40(6):1339–43.

[11] Sierra C, Vazquez AJ. NiAl coatings on carbon steel by self-propagating high-temperature synthesis assisted with concentrated solar energy: mass influence on adherence and porosity. Sol Energy Mater Sol Cells 2005;86(1):33–42.

[12] Sierra C, Vazquez AJ. NiAl coating on carbon steel with an intermediate Ni gradient layer. Surf Coat Technol 2006;200(14–15):4383–8.

[13] Khedari J, Maneewan S, Pratinthong N, Chimchaveed W, Hirunlabhe J. Domestic hot water system combining solar and waste heat from thermoelectric air-conditioner. Int J Ambient Energy 2001;22:19–28.

[14] Maneewan S, Khedari J, Lertsatitthanakorn C, Hirunlabh J. Economical feasibility study of solar hot water system combining waste heat from thermoelectric air-conditioner. In: Proceeding of the 15th ME-NETT Conference, Thailand, October; 2001. p. 68–72.

[15] Yu C, Chau KT. Thermoelectric automotive waste heat energy recovery using maximum power point tracking. Energy Convers Manage 2009;50:1506–12.

[16] Karri MA, Thacher EF, Helenbrook BT. Exhaust energy conversion by thermoelectric generator: two case studies. Energy Convers Manage 2011;52:1596–611.

[17] Telkes M. Solar thermoelectric generators. J Appl Phys 1954;25:765–77.

[18] Maneewan S, Khedari J, Zeghmati B, Hirunlabh J, Eakburanawat J. Investigation on generated power of thermoelectric roof solar collector. Renew Energy 2004;29:743–52.

[19] Champier D, Bedecarrats JP, Rivaletto M, Strub F. Thermoelectric power generation from biomass cook stoves. Energy 2010;35:935–42.

[20] Nuwayhid RY, Shihadeh A, Ghaddar N. Development and testing of a domestic woodstove thermoelectric generator with natural convection cooling. Energy Convers Manage 2005;46:1631–43.

[21] Kraemer D, Poudel B, Feng HP, Caylor JC, Yu B, Yan X, et al. High-performance flat-panel solar thermoelectric generators with high thermal concentration. Nat Mater 2011;10:532–8.

[22] He W, Su YH, Riffat SB, Hou JX, Ji J. Parametrical analysis of the design and performance of a solar heat pipe thermoelectric generator unit. Appl Energy 2011;88:5083–9.

[23] He W, Su YH, Wang YQ, Riffat SB, Ji J. A study on incorporation of thermoelectric modules with evacuated-tube heat-pipe solar collectors. Renew Energy 2012;37:142–9.

[24] Omer SA, Infield DG. Design optimization of thermoelectric devices for solar power generation. Sol Energy Mater Sol Cells 1998;53:67–82.

[25] Omer SA, Infield DG. Design and thermal analysis of a two stage solar concentrator for combined heat and thermoelectric power generation. Energy Convers Manage 2000;41:737–56.

[26] Atik K. Numerical simulation of a solar thermoelectric generator. Energy Source Part A 2011;33:760–7.

[27] Xiao JS, Yang TQ, Li P, Zhai PC, Zhang QJ. Thermal design and management for performance optimization of solar thermoelectric generator. Appl Energy 2012;93:33–8.

[28] Chen G. Theoretical efficiency of solar thermoelectric energy generators. J Appl Phys 2011;109:104908-1–8.

[29] Lesage FJ, Pelletier R, Fournier L, Sempels EV. Optimal electrical load for peak power of a thermoelectric module with a solar electric application. Energy Convers Manage 2013;74:51–9.

[30] www.thermonamic.com/TEP1-12656-0.6-English.pdf.

[31] Beeby S, White NM. Energy harvesting for autonomous systems. Artech House; 2010.